

Ultra-Fast All-Optical Half Subtractor Based on Photonic Crystal Ring Resonators

Atefeh Mirali¹, Mohammad Soroosh^{*1}, Ebrahim Farshidi¹

¹ Department of Electrical Engineering, Shahid Chamran University of Ahvaz, Ahvaz, Iran

(Received 14 Dec. 2019; Revised 20 Jan. 2020; Accepted 17 Feb. 2020; Published 15 Mar. 2020)

Abstract: In this paper, we aim to design and propose a novel structure for all-optical half subtractor based on the photonic crystal. The structure includes two optical switches, one power splitter, and one power combiner. The optical switches are made of the resonant rings which use the nonlinear rods for dropping operation. The footprint of the designed structure is about $602 \mu\text{m}^2$ that is more compact than one in most works. Furthermore, despite some works, the input signals are the same in the phase angle and the optical power. Also, each input signal is applied to one port while this issue has not been considered in some works. Plane wave expansion and finite difference time domain methods are used to calculate the band diagram and simulation of the optical wave propagation throughout the structure, respectively. The maximum obtained rise time of all states of the proposed device is just about 1.4 ps. Besides, the presented structure is capable of working at the third communication window so it can be matched with optical fiber transmission systems.

Keywords: Kerr Effect, Optical Devices, Photonic Bandgap, Photonic Crystal, Subtractor.

1. INTRODUCTION

Photonic crystals (PhCs) [1, 2] are the periodic arrays composed of two or more dielectric materials with different refractive indices. These structures have photonic band gaps (PBGs) where the optical waves have not been allowed for propagation inside the crystal [3, 4]. It has been shown that PhCs can be used for designing a large variety of all-optical devices such as self-collimated waveguides [5–7], filters [8–11], demultiplexers [12–14], logic gates [15–19], adders [20–24], decoders [25–29], encoders [30–33] and [34–39] analog to digital converters.

Optical half subtractors are one of the important building blocks used in all-optical signal processing systems. Optical signal processing systems are required for increasing the speed and bandwidth in communication networks. A PhC-

based half subtractor was proposed by Jiang et al [40] which worked in the self-collimation regime. They used the silicon rods in air background for a hexagonal lattice in which the lattice constant and the diameter of rods were 520.8 nm and 187.5 nm respectively. Two-line defects with the dielectric constant of 1 and 10.4 were inserted to obtain the equal frequency contours for the first band along the Γ -M direction. They used two input powers with different phase angles. To achieve the correct operation of the structure, they assumed the same dielectric constant for both line defects and claimed that the “Borrow” output port was correctly worked in this case. Maximum and minimum of the normalized output power level for logic 0 and 1 were calculated by 7% and 67% respectively. Bakhtiar et al [41] proposed a structure including four adjacent waveguides to obtain the half subtractor operation. By adjusting the refractive indices and proper length of the waveguides, they succeeded in achieving the correct operation. The gap between the normalized output powers for logic 0 and 1 was equal to 10% which is less than one in other works.

Another optical subtractor was presented by Parandin et al [42]. In this work, 19×19 array of dielectric rods with the relative permittivity of 10.4 in air background were inserted in a triangular lattice. The lattice constant and radii of rods were $a=640\text{nm}$ and $r=0.2a$ respectively. They used two cross-connected waveguides and three defects with $r=0.1a$ at the center of the intersection. The difference of phase angle for two incoming signals was equal to 20° and the amount of optical powers in the input ports were not the same. The maximum and minimum values of the normalized output power for logic 0 and 1 were obtained 17% and 67% respectively. They reported that the delay time of the structure was less than 1 ps. Recently, Sivaranjani et al [43] have proposed a triangular PhC lattice as the half subtractor which includes two cross-connect waveguides the same as Ref [42]. The fundamental structure includes a 19×19 array of silicon rods with $r=0.2a$ and defect rods with $r=0.09a$. They calculated 25% and 75% for maximum and minimum values of the normalized output power as logic 0 and 1 respectively. In this research, the time analysis of the structure was not reported.

Based on three x-shape cross-connected waveguides, another structure has been proposed by Moradi [44]. This structure composed of six waveguides and one bias signal to activate the desired ports for different working states. Due to the two-dimensional designing, one of the inputs (as named Y) was applied to two ports that take into account a disadvantage to extend the structure for more bits. The maximum delay time was reported as 3 ps. Recently, Askarian et al [45] have proposed a PhC-based structure using the phase shift technique in waveguides. They guided the input signals in the waveguides with different lengths and combined them to obtain the desired interference patterns in response to the different working states. They reported 2 ps and 66% for the delay time and

the gap between the aforementioned logics, respectively. Also, they have presented another structure using a nonlinear ring resonator in which the optical signal can be dropped in response to the incoming optical intensity in the ring [46]. The delay time and the mentioned gap of the structure were equal to 2 ps and 70%, respectively. The input signals were applied to two ports of the device that is a disadvantage for developing to more bit applications.

In this paper, we are going to design and propose a novel all-optical half subtractor using nonlinear PhC-based ring resonators. It is not concluded any bias signal so the needed optical power is reduced compared with some works. Despite [44-46], the input signals have been applied to the proportional ports in which the extension of the structure for more bit applications be possible. Despite [42,43], input signals of the proposed structure are the same in phase angle and power so this structure has less challenge than [42,43] for employing in the cascaded optical devices. This issue will be amplified when the multiple couplings occur among the devices. The rise time of this structure is about 1.4 ps which is suitable for ultra-fast processing. Besides, the designed device is smaller than [40,41,44-46]. In comparison to other works [40-46] and based on the obtained results, it seems the proposed structure can be used as a fundamental structure for half subtractors.

The next sections were organized as follows: in section 2, the design procedure of the proposed switches will be introduced. Then, the PhC-based half subtractor is presented in section 3. Simulation of the structure and discussions will be presented in section 4. The final section includes the conclusion of this study.

2. OPTICAL SWITCHES

The fundamental PhC structure is a two-dimensional square lattice of InP rods in which the refractive index and radius are 3.1 and 226 nm, respectively. Also, the lattice constant or spatial period of the crystal is 630 nm. The plane wave expansion method is used to calculate the band diagram [47]. In this method, Maxwell's equations are written as the following:

$$\frac{1}{\epsilon_r} \nabla \times \nabla \times E = \left(\frac{\omega}{c}\right)^2 E \quad (1)$$

$$\nabla \times \frac{1}{\epsilon_r} \nabla \times H = \left(\frac{\omega}{c}\right)^2 H \quad (2)$$

where ϵ_r is the relative permittivity, c is the speed of light in vacuum and ω is the frequency of optical waves. Using Fourier series expansions for electric (E) and magnetic (H) fields, the eigenvalues $(\omega/c)^2$ are obtained for different wave vectors. Figure 1 shows that the fundamental structure has two PBGs for TE and TM modes. The calculated PBG for TM mode is at $0.32 < a/\lambda < 0.44$ where a and λ are the lattice constant and wavelength, respectively. In respect of the

mentioned value for a , the photonic bandgap of the structure is at $1432 \text{ nm} < \lambda < 1969 \text{ nm}$ for TM mode. This wide interval covers the third optical communication window included C and L bands, so the structure is capable of using for optical communication applications.

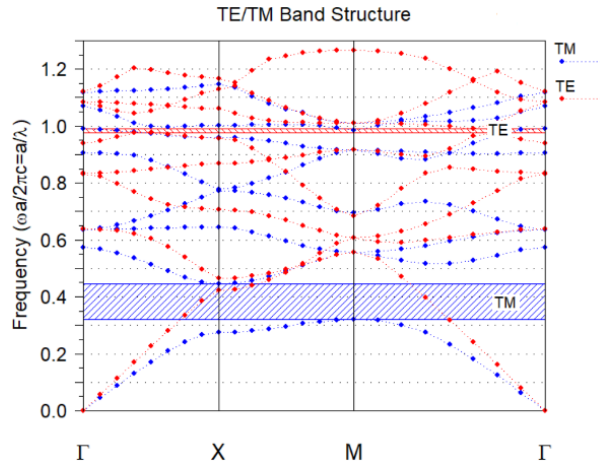


Fig. 1. The band diagram of the fundamental structure.

To design the half subtractor, two switches named as S1 and S2 including the nonlinear resonant rings are used. The first switch (or S1) is shown in figure 2a, in which a nonlinear ring is located between two parallel waveguides. The red and dark blue circles present the fundamental and defect rods. The port A is assumed as the input of the switch and hence the incoming optical waves could be propagated toward the ports B, C, and D. To approach the nonlinear regime, a control port is used for increasing the optical intensity in the resonant ring. In the following, the role of this port will be shown. The nonlinear rods are made of the chalcogenide glass with the nonlinear refractive index of $9 \times 10^{-17} \text{ m}^2/\text{W}$ [48]. By incoming a pulse to port A, the transmission of each output port is obtained for different harmonics as shown in figure 2b. It can be seen that the resonant mode of the ring is occurred at about 1547 nm. On the other hand, the optical waves with the resonant mode have phase angle difference equal to $2m\pi$ where m is an integer number (e.g. $m=1,2,3,\dots$) [47]. So, the constructive interferences occur in the resonant mode. In this case, optical waves from the upper waveguide drop to the lower waveguide and reach to the port C.

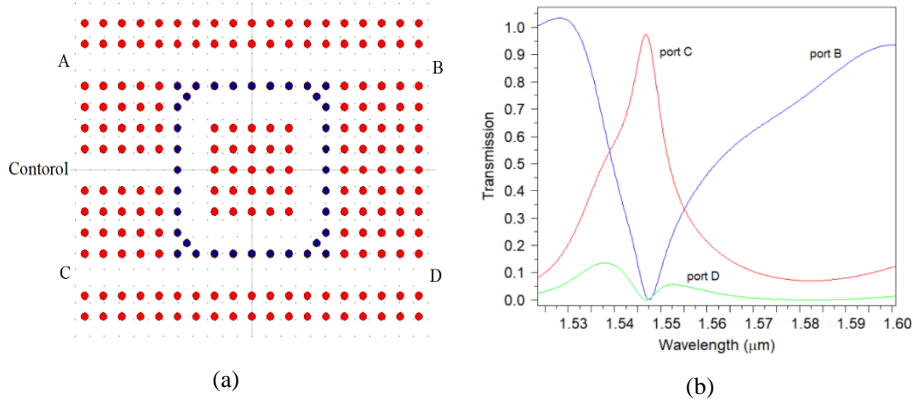


Fig. 2. (a) The proposed structure and (b) the mode analysis of the switch S1.

The output ports were swept for different values of the incoming optical intensities for control port. It demonstrated that the threshold intensity for switch S1 is about $1.2 \text{ mW}/\mu\text{m}^2$. The threshold value is obtained when the optical intensity of port B be equal to that for port C. Figure 3 shows the optical wave propagation through the switch S1 for both control intensities, $I_c=0.5 \text{ mW}/\mu\text{m}^2$ and $I_c=1.5 \text{ mW}/\mu\text{m}^2$. In the first case, the amount of the intensity is lower than the mentioned threshold intensity so the resonant ring drops the optical waves toward the port C.

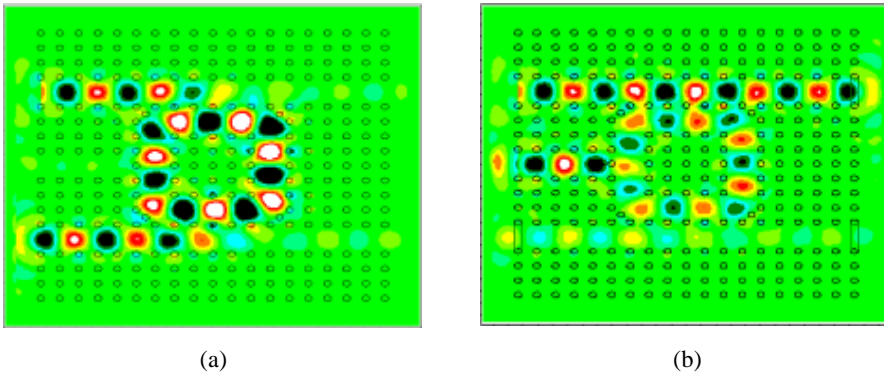


Fig. 3. The optical waves propagation in the switch S1 for two cases (a) $I_c=0.5 \text{ mW}/\mu\text{m}^2$ and (b) $I_c=1.5 \text{ mW}/\mu\text{m}^2$.

For $I_c=1.5 \text{ mW}/\mu\text{m}^2$, the high optical intensity is introduced in the resonant ring, so the effective refractive index and hence the resonant mode of the ring will be changed. This issue is known as the Kerr effect in which the refractive index of a dielectric material (n) depends on the incident optical intensity (I). This effect

is defined as $n(I)=n_1+n_2I$ where n_1 is the linear refractive index and n_2 is the nonlinear coefficient [48]. In this case, the resonant mode of the ring is not matched with the wavelength of the entered optical signal, so the optical waves are not dropped to the lower waveguide.

The structure of the switch S2 is shown in figure 4a. All parameters of this switch are similar to the first one, however, the control port of the switch has been deleted. The mode analysis of the structure is presented in figure 4b. It can be concluded the resonant mode of the switch S2 is very near the one for S1.

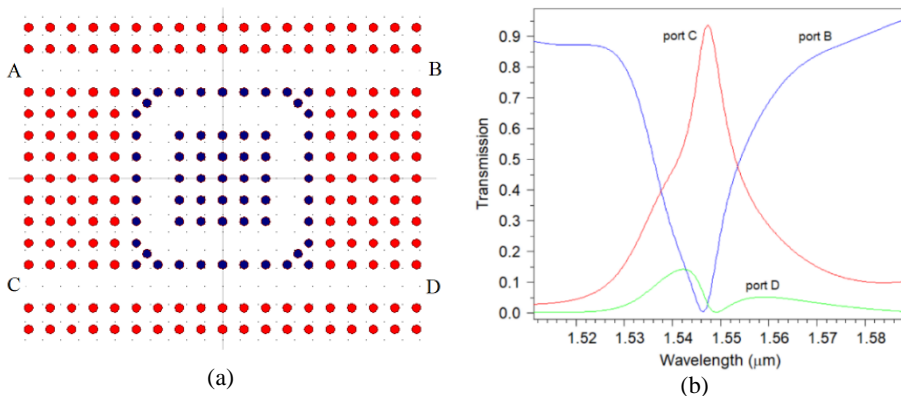


Fig. 4. (a) The schematic and (b) mode analysis for the switch S2.

Using an optical signal with wavelength 1547 nm, different optical intensities are introduced from port A and the threshold intensity for the switching is achieved about $1 \text{ mW}/\mu\text{m}^2$. As shown in figure 5, simulation results demonstrate that for the optical intensities which are lower than the threshold value (for example $I=0.5 \text{ mW}/\mu\text{m}^2$) the dropping is carried out while it can't be done for ones higher than the threshold (for example $I=1.5 \text{ mW}/\mu\text{m}^2$).

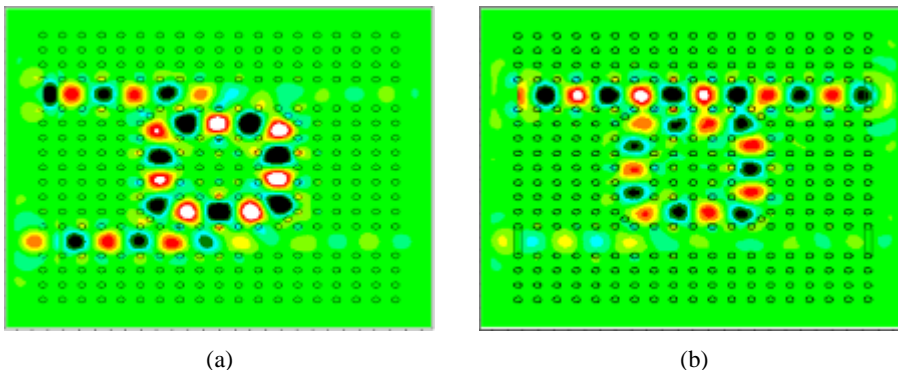


Fig. 5. Distribution of the optical waves for switch S2 in which the entered optical power is (a) lower and (b) higher than the threshold value for switching.

3. OPTICAL HALF SUBTRACTOR

The proposed optical half subtractor is designed by combining the optical switches that were introduced in section 2. As shown in figure 6, the structure includes ports X and Y as the inputs and ports B and D as the outputs. Five waveguides (named as W1, W2, W3, W4, and W5) were used to guide the incoming optical signals toward the output ports. Input signal Y is reached to a splitter through waveguide W2 and the amount of optical power is divided into two equal parts. The first part is guided through waveguide W4 toward the resonant ring R2. Based on the incoming optical power into the ring, the signal can be dropped toward the port B. Another part is transmitted via waveguide W3 and is combined with the introduced signal from port X. Waveguide W1 guides the applied signal to port X toward an optical combiner. Interference of them is guided toward the resonant ring R1 through waveguide W5. According to the optical Kerr effect, the optical waves can be dropped toward the port D and activate it.

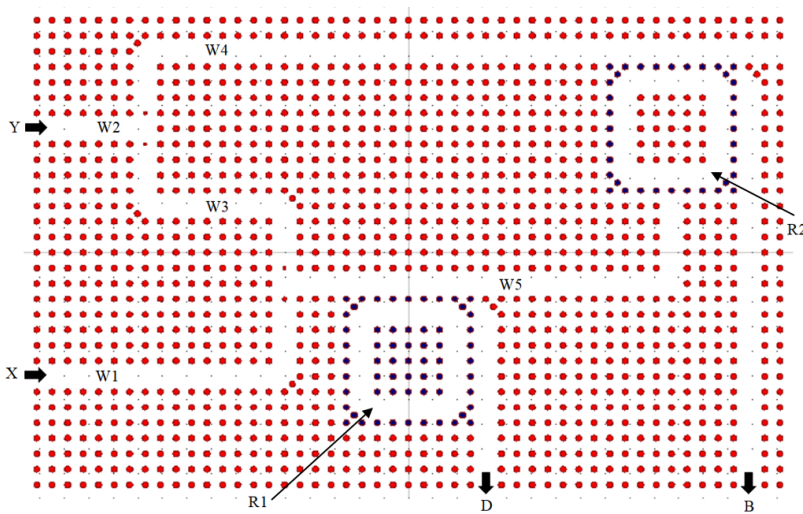


Fig. 6. The proposed structure for all-optical half subtractor.

For solving Maxwell's equations and simulation of the light propagation throughout the structure, the finite difference time domain method is used. In this method, the electric and magnetic fields are calculated based on Yee's unit cell in space and time [47]. The length of the unit cell in both x and z directions, Δx and Δz , should be smaller than $\lambda/10$ so they are assumed by 100 nm. The components of the fields should be calculated in distance of $\Delta x/2$ and $\Delta z/2$ in space. Besides, the time step (Δt) is determined by the Courant condition as follow:

$$c\Delta t < \frac{1}{\sqrt{\left(\frac{1}{\Delta x^2} + \frac{1}{\Delta z^2}\right)}} \quad (3)$$

According to this condition, the time step is assumed by 80 fs. It is obvious that when both input ports are OFF, there is no signal in the structure so both output ports will be OFF (figure 7a). When X is ON and Y is OFF, R1 drops the optical waves from W5 into the output waveguide. Therefore, the optical waves reach the port D while they won't be appeared at the port B. As a result, in this case, D is ON and B is OFF (figure 7b). If X becomes OFF while Y is ON, R1 and R2 drop the optical waves from W5 and W4 into the output waveguides. So, the optical waves reach to the ports D and B and they become ON (figure 7c). When both input ports are ON, due to the high amount of optical intensity into the resonant rings, none of them drop the optical waves from W4 and W5 into the output ports. In this case, no optical waves reach the output ports and hence they will be OFF (figure 7d).

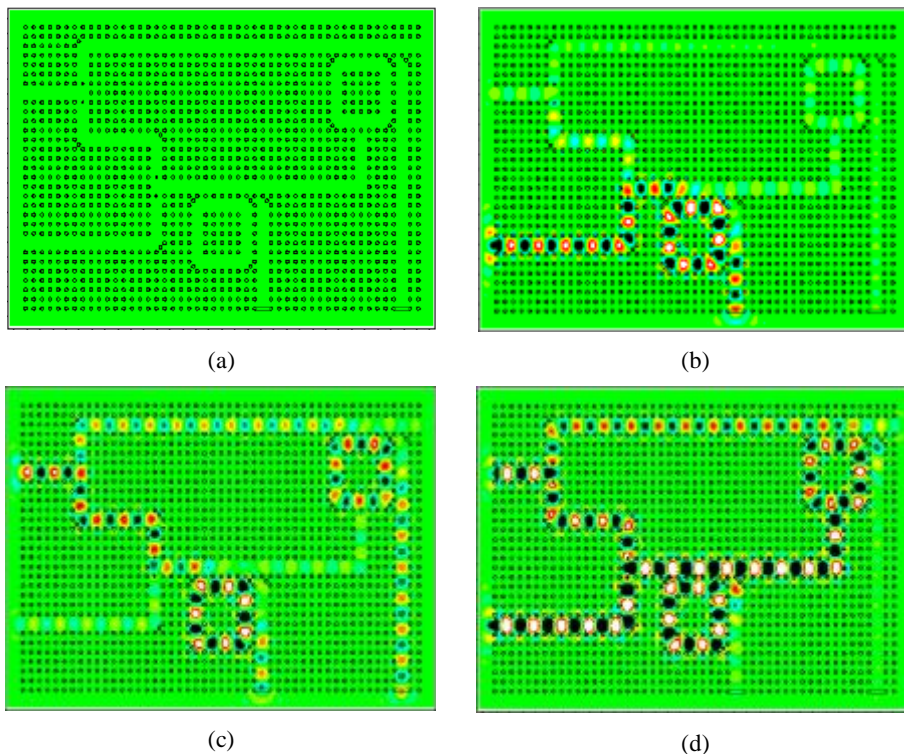


Fig. 7. The optical waves propagation in the structure for (a) X=Y=0, (b) X=1, Y=0, (c) X=0, Y=1, (d) X=Y=1.

As can be inferred, the proposed structure can correctly guide the input optical waves toward the desired waveguides so the subtracting operation is achieved. For more evaluating the structure, it is necessary that the time response is calculated too. Figure 8 depicts the time response of the structure for all possible states. Proportional to the figure 7a, no optical power is reported for output ports as shown in figure 8a. The amount of the normalized power at ports D and B will be 64% and 5%, respectively for $X=1$ and $Y=0$ (figure 8b). In this case, the rise time for port D is about 1 ps. In this study, the rise time is defined as the time where the power reaches 90% steady-state value. As shown in figure 8c, the amount of the normalized output power at both ports D and B will be 41% and the rise time is about 1 ps. The normalized power at output ports D and B will be obtained by about 5% and 3%, respectively which are proportional to figure 7d (figure 8d). In this case, the rise time is calculated by about 1.4 ps.

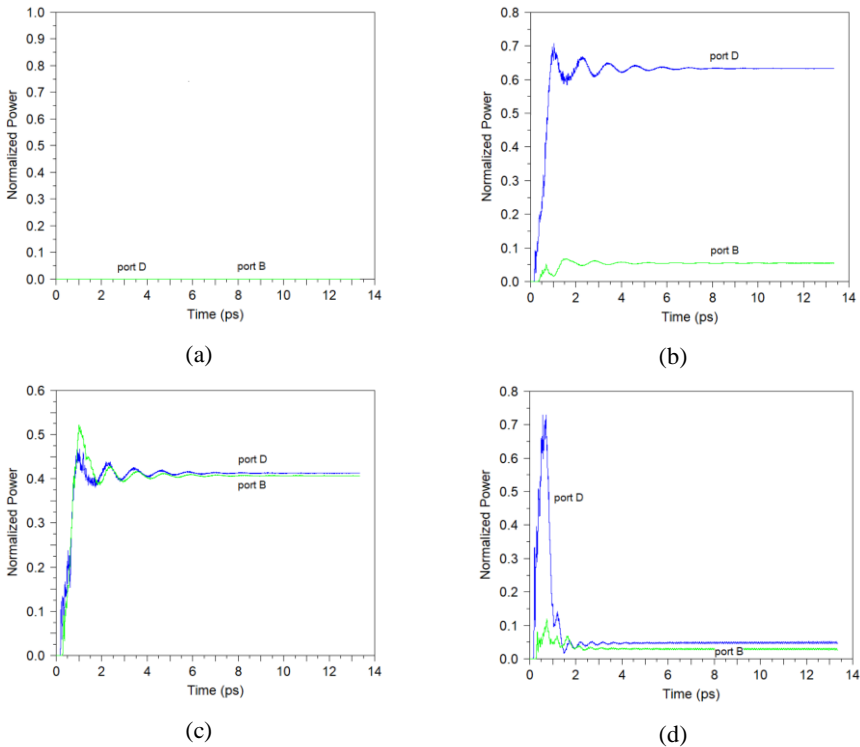


Fig. 8. The time response of the presented device for (a) $X=Y=0$, (b) $X=1, Y=0$, (c) $X=0, Y=1$, (d) $X=Y=1$.

Table I summarizes the obtained results of time analysis for the proposed PhC-based half subtractor. The maximum rise time of the output ports for all input states is obtained by 1.4 ps which is corresponding to 714 GHz. It can be seen that the maximum normalized power for logic 0 and the minimum normalized power for logic 1 are equal to 5% and 41%, respectively. For the presented structure, these values are assumed as the logic margins.

TABLE I
THE CALCULATED RESULTS FOR TIME ANALYSIS.

Input ports		Normalized output power (logic)		Rise time(ps)
X	Y	D	B	
0	0	- (0)	- (0)	-
1	0	64% (1)	5% (0)	1
0	1	41% (1)	41% (1)	1
1	1	5% (0)	3% (0)	1.4

The above-mentioned analysis for time response in addition to the optical wave transmission throughout the structure demonstrate the proposed half subtractor is capable of using in optical processing applications. To have a better assessment of the proposed device, the simulation results have been compared with ones for other works in Table II. It includes the important factors such as the footprint (FP), the rise time (Tr), the optical intensity (I), the gap between the margins for logic 0 and 1 (G), and the type of the working regime. The symbol “-” shows no value is reported in the references.

TABLE II
Comparison of the obtained results in this work with ones in other works.

Works	FP (μm^2)	Tr (ps)	I ($\text{mW}/\mu\text{m}^2$)	G (%)	Working regime
[40]	668	-	-	60	self-collimation
[41]	16×10^3	-	3×10^3	10	Nonlinear
[42]	148	1	-	50	Linear
[43]	138	-	1	50	Linear
[44]	709	3	100	60	Nonlinear
[45]	674	1	10^4	66	Nonlinear
[46]	946	2	1	70	Linear
This work	602	1.4	1.5	36	Nonlinear

It can be seen that the footprint of the proposed structure is less than one in other works except for [42,43]. The presented structure includes two same input signals at phase angle and power while they are different in [42,43]. This issue will be more important when multiple couplings occur between two devices or

stages in optical circuits. In this case, the power margins for a device must be set in the allowed ones for the next device. Furthermore, each deviation in the fabrication process affects directly the phase angle of propagating waves in waveguides so the device operation may be disrupted. This problem is inherently included in structures whose inputs are different at phase angle such as [42,43].

In [44-46], two ports are simultaneously supposed for an optical signal such as X or Y. Although this issue is considered to overcome the two-dimensional confinements, the extension of the mentioned structure for more bit applications has serious difficulties. Besides, to approach the correct operation in [44,46], the bias signals have been added to the structure. This idea has been used to enhance the value of the gap between the margins for logic 0 and 1. As far as we know, employing the extra optical signals in designing increases the power consumption of the structure so using these signals takes into account a disadvantage for the mentioned references.

In [40], the presented device works in self-collimation regime in which the selection of equal frequency contour is very sensitive to the structural parameters. On the other hand, the small deviation of the structural parameters from the desired values decreases the performance of the device. Employing the parallel waveguides and using the nonlinear coupling in [41] results in a large area for designing the half subtractor.

According to the mentioned discussions, it seems the proposed device can be used in optical processing circuits. The designed half subtractor is capable of considering as a fundamental structure to design the more bit applications.

4. CONCLUSION

In this study, an all-optical half subtractor based on photonic crystal structure has been presented. The structure consists of two switches, a power combiner and a beam splitter. The chalcogenide rods as nonlinear materials are placed in the both switches. Considering the nonlinear Kerr effect, the resonant rings only drop the optical waves for low power regimes. The time analysis of the structure demonstrates values 5% and 41% for low and high-level margins, respectively. Furthermore, the rise time of the proposed device is calculated by about 1.4 ps. Besides, the input ports are launched by the optical waves which are at the same. The correct operation of the structure in addition to the aforementioned results demonstrate that the proposed device can be included in optical circuits.

REFERENCES

- [1] S. John, *Strong localization of photons in certain disordered dielectric superlattices*, Phys. Rev. Lett. 58(23) (1987) 2486-2489. Available: <https://journals.aps.org/prl/abstract/10.1103/PhysRevLett.58.2486>

- [2] E. Yablonovitch, *Inhibited spontaneous emission in solid-state physics and electronics*, Phys. Rev. Lett. 58(20) (1987) 2059–2062. Available: <https://journals.aps.org/prl/abstract/10.1103/PhysRevLett.58.2059>
- [3] D. Liu, Y. Gao, A. Tong, and S. Hu, *Absolute photonic band gap in 2D honeycomb annular photonic crystals*, Phys. Lett. A. 379(3) (2015) 214–217.
Available: <https://www.sciencedirect.com/science/article/pii/S0375960114011591>
- [4] H. Alipour-Banaei and F. Mehdizadeh, *Bandgap calculation of 2D hexagonal photonic crystal structures based on regression analysis*, J. Opt. Commun. 34(4) (2013) 285–293.
Available: <https://www.degruyter.com/view/j/joc.2013.34.issue-4/joc-2013-0033/joc-2013-0033.xml>
- [5] M. Noori, M. Soroosh, and H. Baghban, *Highly efficient self-collimation based waveguide for Mid-IR applications*, Photonics Nanostructures Fundam. Appl. 19 (2016) 1–11.
Available: <https://www.sciencedirect.com/science/article/pii/S1569441016000067>
- [6] M. Noori and M. Soroosh, *A comprehensive comparison of photonic band gap and self-collimation based 2D square array waveguides*, Opt. Int. J. Light Electron Opt. 126(23) (2015) 4775–4781. Available: <https://www.sciencedirect.com/science/article/pii/S0030402615008438>
- [7] Y. A. Vlasov, M. O’Boyle, H. F. Hamann, and S. J. McNab, *Active control of slow light on a chip with photonic crystal waveguides*, Nature 438 (2005) 65–69. Available: <https://www.nature.com/articles/nature04210>
- [8] G. Moloudian, R. Sabbaghi-Nadooshan, and M. Hassangholizadeh-Kashtiban, *Design of all-optical tunable filter based on two-dimensional photonic crystals for WDM (wave division multiplexing) applications*, J. Chinese Inst. Eng. Trans. Chinese Inst. Eng. A., 39(8) (2016) 971–976.
Available: <https://www.tandfonline.com/doi/abs/10.1080/02533839.2016.1215937?journalCode=tcie20>
- [9] M. Zamani, *Photonic crystal-based optical filters for operating in second and third optical fiber windows*, Superlattices Microstruct. 92 (2016) 157–165.
Available: <https://www.sciencedirect.com/science/article/pii/S0749603616300684>

- [10] V. Fallahi and M. Seifouri, *Novel structure of optical add/drop filters and multi-channel filter based on photonic crystal for using in optical telecommunication devices*, J. Optoelectro. Nanostruc. 4(2) (2019) 53-68. Available: http://jopn.miau.ac.ir/article_3478.html
- [11] Z. Rashki, S. J. S. Mahdavi Chabok, *Novel Design for Photonic Crystal Ring Resonators Based Optical Channel Drop Filter*, J. Optoelectro. Nanostruc. 3(3) (2018) 59-78. Available: http://jopn.miau.ac.ir/article_3046.html
- [12] V. Kannaiyan, R. Savarimuthu, and S. K. Dhamodharan, *Investigation of 2D-photonic crystal resonant cavity based WDM demultiplexer*, Opto-Electronics Rev. 26(2) (2018) 108-115.
Available:
<https://www.sciencedirect.com/science/article/pii/S1230340217300951>
- [13] E. Rafiee and F. Emami, *Design of a novel all-optical ring shaped demultiplexer based on two-dimensional photonic crystals*, Opt. Int. J. Light Electron Opt. 140 (2017) 873-877.
Available:
<https://www.sciencedirect.com/science/article/pii/S0030402617305326>
- [14] R. Talebzadeh, M. Soroosh, Y.S. Kaviani, and F. Mehdizadeh, *Eight-channel all-optical demultiplexer based on photonic crystal resonant cavities*, Opt. Int. J. Light Electron Opt., 140 (2017) 331-337. Available: <https://www.sciencedirect.com/science/article/pii/S0030402617304795>
- [15] H. Alipour-Banaei, S. Serajmohammadi, and F. Mehdizadeh, *All optical NAND gate based on nonlinear photonic crystal ring resonators*, Opt. Int. J. Light Electron Opt. 130 (2017) 1214-1221. Available: <https://www.sciencedirect.com/science/article/pii/S0030402616315261>
- [16] A. Kumar, M. M. Gupta, and S. Medhekar, *All-optical NOT and AND gates based on 2D nonlinear photonic crystal ring resonant cavity*, Opt. Int. J. Light Electron Opt. 179 (2019) 239-247. Available: <https://www.sciencedirect.com/science/article/pii/S003040261831711X>
- [17] N. F.F. Areed, A. El Fakharany, M. F.O. Hameed, and S. S. A. Obayya, *Controlled optical photonic crystal AND gate using nematic liquid crystal layers*, Opt. Quantum Electron. 49 (2017) 45-53. Available: <https://link.springer.com/article/10.1007/s11082-016-0852-z>
- [18] T. A. Moniem, *All-optical XNOR gate based on 2D photonic-crystal ring resonators*, Quantum Electron. 47(2) (2017) 169-176. Available: <http://adsabs.harvard.edu/abs/2017QuEle..47..169M>

- [19] F. Mehdizadeh and M. Soroosh, *Designing of all optical NOR gate based on photonic crystal*, Indian J. Pure Appl. Phys. 54 (2016) 35-39. Available: <http://op.niscair.res.in/index.php/IJPAP/article/view/5678/576>
- [20] M. Neisy, M. Soroosh, and K. Ansari-Asl, *All optical half adder based on photonic crystal resonant cavities*, Photonic Netw. Commun. 35(2) (2018) 245-250. Available: <https://link.springer.com/article/10.1007/s11107-017-0736-6>
- [21] M. R. Jalali-Azizpoor, M. Soroosh, and Y. Seifi-Kavian, *Application of self-collimated beams in realizing all-optical photonic crystal-based half-adder*, Photonic Netw. Commun. 36(3) (2018) 344-343. Available: <https://link.springer.com/article/10.1007/s11107-018-0786-4>
- [22] F. Cheraghi, M. Soroosh, and G. Akbarizadeh, *An ultra-compact all optical full adder based on nonlinear photonic crystal resonant cavities*, Superlattices Microstruct. 113 (2018) 359-365. Available: <https://www.sciencedirect.com/science/article/pii/S0749603617322826>
- [23] S. Serajmohammadi, H. Alipour-Banaei, and F. Mehdizadeh, *Proposal for realizing an all-optical half adder based on photonic crystals*, Appl. Opt. 57(7) (2018) 1617-1621.
Available: <https://www.osapublishing.org/ao/abstract.cfm?URI=ao-57-7-1617>
- [24] A. Rahmani and F. Mehdizadeh, *Application of nonlinear PhCRRs in realizing all optical half-adder*, Opt. Quantum Electron. 50 (2017) 30-37. Available: <https://link.springer.com/article/10.1007/s11082-017-1301-3>
- [25] T. Daghooghi, M. Soroosh, and K. Ansari-Asl, *A low-power all optical decoder based on photonic crystal nonlinear ring resonators*, Opt. Int. J. Light Electron Opt. 174 (2018) 400-408. Available: <https://www.sciencedirect.com/science/article/pii/S0030402618312397>
- [26] F. Mehdizadeh, H. Alipour-Banaei, and S. Serajmohammadi, *Design and simulation of all optical decoder based on nonlinear PhCRRs*, Opt. Int. J. Light Electron Opt. 156 (2018) 701-706. Available: <https://www.sciencedirect.com/science/article/pii/S003040261731639X>
- [27] T. Daghooghi, M. Soroosh, and K. Ansari-Asl, *Ultra-fast all-optical decoder based on nonlinear photonic crystal ring resonators*, Appl. Opt. 57(9) (2018) 2250-2257.
Available: <https://www.osapublishing.org/ao/abstract.cfm?URI=ao-57-9-2250>

- [28] F. Mehdizadeh, H. Alipour-banaei, and S. Serajmohammadi, *Study the role of non-linear resonant cavities in photonic crystal-based decoder switches*, J. Mod. Opt. 64(13) (2017) 1233-1239.

Available:

<https://www.tandfonline.com/doi/abs/10.1080/09500340.2016.1275854>

- [29] T. A. Moniem, *All optical active high decoder using integrated 2D square lattice photonic crystals*, J. Mod. Opt. 62(19) (2015) 1643-1649. Available: <https://www.tandfonline.com/doi/abs/10.1080/09500340.2015.1061061?journalCode=tmop20>

- [30] F. Haddadan and M. Soroosh, *Low-power all-optical 8-to-3 encoder using photonic crystal-based waveguides*, Photonic Netw. Commun. 37(1) (2018) 67-73. Available: <https://link.springer.com/article/10.1007/s11107-018-0795-3>

- [31] F. Mehdizadeh, M. Soroosh, and H. Alipour-Banaei, *Proposal for 4-to-2 optical encoder based on photonic crystals*, IET Optoelectron. 11(1) (2017) 29-35.

Available: <https://digital-library.theiet.org/content/journals/10.1049/iet-opt.2016.0022>

- [32] A. Salimzadeh and H. Alipour-Banaei, *An all optical 8 to 3 encoder based on photonic crystal OR-gate ring resonators*, Opt. Commun. 410 (2018) 793-798.

Available:

<https://www.sciencedirect.com/science/article/pii/S0030401817310544>

- [33] T. A. Moniem, *All-optical digital 4×2 encoder based on 2D photonic crystal ring resonators*, J. Mod. Opt. 63(8) (2016) 735-741. Available: <https://www.tandfonline.com/doi/abs/10.1080/09500340.2015.1094580?journalCode=tmop20>

- [34] K. Fasihi, *All-optical analog-to-digital converters based on cascaded 3-dB power splitters in 2D photonic crystals*, Opt. Int. J. Light Electron Opt. 125 (2014) 6520-6523.

Available:

<https://www.sciencedirect.com/science/article/pii/S0030402614009784>

- [35] F. Mehdizadeh, M. Soroosh, H. Alipour-Banaei, and E. Farshidi, *A novel proposal for all optical analog-to-digital converter based on photonic crystal structures*, IEEE Photonics J. 9(2) (2017) 4700311-4700322. Available: <https://ieeexplore.ieee.org/stamp/stamp.jsp?arnumber=7891002>

- [36] F. Mehdizadeh, M. Soroosh, H. Alipour-Banaei, and E. Farshidi, *All optical 2-bit analog to digital converter using photonic crystal based cavities*, Opt. Quantum Electron. 49 (2017) 38-45. Available: <https://link.springer.com/article/10.1007/s11082-016-0880-8>
- [37] F. Mehdizadeh, M. Soroosh, H. Alipour-Banaei, and E. Farshidi, *Ultra-fast analog-to-digital converter based on a nonlinear triplexer and an optical coder with a photonic crystal structure*, Appl. Opt. 56(7) (2017) 1799-1806. Available: <https://www.osapublishing.org/ao/abstract.cfm?uri=ao-56-7-1799>
- [38] A. Tavousi and M. A. Mansouri-Birjandi, *Optical-analog-to-digital conversion based on successive-like approximations in octagonal-shape photonic crystal ring resonators*, Superlattices Microstruct. 114 (2018) 23-31.
Available: <https://www.sciencedirect.com/science/article/pii/S0749603617323273>
- [39] A. Tavousi, M. A. Mansouri-Birjandi, and M. Saffari, *Successive approximation-like 4-bit full-optical analog-to-digital converter based on Kerr-like nonlinear photonic crystal ring resonators*, Phys. E Low-dimensional Syst. Nanostructures, 83(?) (2016) 101-106. Available: <https://www.sciencedirect.com/science/article/pii/S1386947716301795?via%3Dihub>
- [40] Y. C. Jiang, S. B. Liu, H. F. Zhang, and X. K. Kong, *Design of ultra-compact all optical half subtractor based on self-collimation in the two-dimensional photonic crystals*, Opt. Commun., 356 (2015) 325-329. Available: <https://www.sciencedirect.com/science/article/abs/pii/S0030401815006598?via%3Dihub>
- [41] F. Parandin, M. R. Malmir, and M. Naseri, *All-optical half-subtractor with low-time delay based on two-dimensional photonic crystals*, Superlattices Microstruct., 109 (2017) 437-441.
Available: <https://www.sciencedirect.com/science/article/pii/S0749603617309849?via%3Dihub>
- [42] R. Sivaranjani, A. S. Raja, D. S. Sundar, and T. K. Shanthi, *Design of 2-dimensional photonic crystal based all optical half subtractor*, International J. Adv. Eng. Res. Develop. 5(8) (2018) 1-7. Available: http://ijaerd.com/papers/special_papers/NCMOC11.pdf
- [43] H. A. Haus, *Waves and fields in optoelectronics*, Prentice-Hall, Chapter 7, 1984.

- [44] B. Youssefi, M. K. Moravvej-Farshi, and N. Granpayeh, *Two bit all-optical analog-to-digital converter based on nonlinear Kerr effect in 2D photonic crystals*, *Opt. Commun.* 285(13-14) (2012) 3228-3233. Available: <https://www.sciencedirect.com/science/article/abs/pii/S0030401812002349>

